

## ***Bacillus subtilis* CwIP of the SP-beta Prophage has Two Novel Peptidoglycan Hydrolase Domains, Muramidase and Cross-Linkage Digesting D,D-Endopeptidase\*<sup>S</sup>**

**I Putu Sudiarta<sup>§1</sup>, Tatsuya Fukushima<sup>¶1</sup>, and Junichi Sekiguchi<sup>§¶2</sup>**

*From the <sup>§</sup>Interdisciplinary Graduate School of Science and Technology, and <sup>¶</sup>Division of Gene Research, Department of Life Sciences, Research Center for Human and Environmental Sciences, Shinshu University, Nagano 386-8567, Japan*

Running title: Novel cell wall hydrolase in a *B. subtilis* prophage

<sup>1</sup> These authors contributed equally to this work.

<sup>2</sup> To whom correspondence should be addressed: Interdisciplinary Graduate School of Science and Technology, Shinshu University, 3-15-1 Tokida, Ueda 386-8567, Japan. Tel: 81-268-21-5344; Fax: 81-268-21-5345; E-mail: jsekigu@shinshu-u.ac.jp.

For bacteria and bacteriophages, cell wall digestion by hydrolases is a very important event. We investigated one of the proteins involved in cell wall digestion, the *yomI* gene product (renamed CwIP). The gene is located in the SP-beta prophage region of the *Bacillus subtilis* chromosome. Inspection of the Pfam database indicates that CwIP contains soluble lytic transglycosylase (SLT) and peptidase M23 domains, which are similar to *Escherichia coli* lytic transglycosylase Slt70, and the *Staphylococcus aureus* Gly-Gly endopeptidase LytM, respectively. The SLT domain of CwIP exhibits hydrolytic activity towards *B. subtilis* cell wall; however, reverse-phase (RP)-HPLC and mass spectrometry revealed that the CwIP-SLT domain has only muramidase activity. In addition, the peptidase M23 domain of CwIP exhibited hydrolytic activity and could cleave D-Ala-diaminopimelic acid cross-linkage, a property associated with D,D-endopeptidases. Remarkably, the M23 domain of CwIP possessed a unique Zn<sup>2+</sup>-independent endopeptidase activity; this contrasts with all other characterized M23 peptidases (and enzymes similar to CwIP) which are Zn<sup>2+</sup> dependent. Both domains of CwIP could hydrolyze the peptidoglycan and cell wall of *B. subtilis*. However, the M23 domain digested neither the peptidoglycans nor the cell walls of *S. aureus* or *Streptococcus thermophilus*. The effect of defined point mutations in

conserved amino acid residues of CwIP is also determined.

The cycle of bacteriophage infection of microorganisms comprises adsorption, insertion of nucleic acids, production of bacteriophage nucleic acids and proteins, and finally, host cell lysis. The infection cycle follows a highly-ordered sequence of events where cell wall hydrolases, encoded in bacteriophage genomes, are involved in adsorption to cell walls (first infection cycle) and host cell lysis (final infection cycle) (1).

One of the best-studied Gram-positive bacteria, *Bacillus subtilis*, has prophage-like elements including PBSX, skin and SP-beta (2). The SP-beta prophage is the largest prophage-like element in *B. subtilis* (2). Inspection of the BSORF database (<http://bacillus.genome.jp/>) indicates that the SP-beta prophage chromosomal region contains 184 genes and one cell wall hydrolase called BlyA, which has been identified as an L-alanine amidase (3). Interestingly, the Pfam database predicts that another gene product, YomI [renamed CwIP (cell wall lytic enzyme related to phage)], has two cell wall hydrolase domains, a soluble lytic transglycosylase (SLT) and peptidase M23 (Fig. 1).

However, the function of the two domains (SLT and peptidase M23) remains unclear. BLAST searches of the BSORF and Pfam databases indicate that the SLT domain contains a soluble lytic transglycosylase and a muramidase, although the domain name is

annotated “SLT”. At present, lytic transglycosylases and muramidases cannot be differentiated using amino acid sequence similarity. The peptidase M23 domain has hydrolytic activity, enabling it to digest Gly-Gly bond. It is also known that LytM in *Staphylococcus aureus* has a peptidase M23 domain, which has been identified as a glycyl-glycine endopeptidase (4). However, *B. subtilis* LytH also has a peptidase M23 domain and has been shown to digest the L-Ala-D-Glu bond of spore peptidoglycans *in vivo* (5). At present, the activity of peptidase M23 domain of CwIP is unknown. The aim of this study, therefore, was to conduct a biochemical analysis of CwIP to enable us to predict its function.

Here, we report that the SLT domain of CwIP exhibits hydrolase activity towards *B. subtilis* cell wall and can digest the linkage between MurNAc and GlcNAc. The property is characteristic of a muramidase, not a lytic transglycosylase. We determined that the active site for hydrolysis is Glu1447. The M23 domain of CwIP was also found to exhibit hydrolase activity toward *B. subtilis* cell wall as a D,D-endopeptidase, which digests the D-Ala-diaminopimelic acid (A<sub>2</sub>pm) bond of the cross-linkage. The critical amino acid residues in the M23 domain comprise His1628 and His1660. Unusually, the D-alanyl-A<sub>2</sub>pm endopeptidase of the M23 domain of CwIP does not require Zn<sup>2+</sup> ions, but Ca<sup>2+</sup> for enzymatic activity.

## EXPERIMENTAL PROCEDURES

**Bacterial Strains and Plasmids**—The plasmids and primers used in this study are listed in Supplemental Tables S1 and S2, respectively. The *Escherichia coli* strains, JM109 [*recA1*,  $\Delta$ (*lac-proAB*) *endA1*, *gyrA96*, *thi-1*, *hsdR17*, *relA1*, *supE44*, (F' *traD36 proAB*<sup>+</sup>, *lacI*<sup>f</sup>, *lacZ*,  $\Delta$ M15)] and M15 (Nal<sup>s</sup>, Str<sup>s</sup> Rif<sup>s</sup>, *lac ara*, *gal*, *mtl* F<sup>-</sup>, *recA*<sup>+</sup>, *uvr*<sup>+</sup>), used in this study were grown in LB medium (6) at 37°C containing a final concentration of 100 µg/ml ampicillin. If necessary, 2% glucose and 1 mM IPTG were added to the medium. *B. subtilis* 168 (*trpC*) was also grown in LB medium at 37°C.

**Construction of Plasmid pQE-SLT for Over-expression of the SLT Domain of CwIP**—The region containing the SLT domain of CwIP (comprising amino acids 1,424-1,534) was amplified by PCR using BF-SLT and KR-SLT primers (Supplemental Table S2) and *B. subtilis* 168 DNA. The amplified fragments were digested with *Bam*HI and *Kpn*I and ligated to the corresponding digested sites of pUC119, resulting in the plasmid designated pUC-SLT. pUC-SLT was digested with *Bam*HI and *Kpn*I, and the fragment containing the SLT domain was subcloned into pQE-30 (Qiagen), resulting in pQE-SLT. The above construct was used for over-expression of the SLT domain (CwIP-SLT) (Fig. 1).

**Construction of Plasmids for Over-expression of the Peptidase M23 Domain and SLT-peptidase M23 Domain of CwIP**—The region containing the peptidase M23 domain or the SLT-peptidase M23 domain of CwIP was amplified by PCR using BF-M23 and HR-M23 primers or BF-SLT and KR-M23 primers, respectively. *B. subtilis* 168 DNA was used as the template for these reactions. The amplified fragments were digested with *Bam*HI and *Hind*III and ligated to the corresponding digested sites of pQE-30, resulting in pQE-M23 (peptidase M23 domain) and pQE-SLTM23 (SLT-peptidase M23 domain). These constructs were used for over-expression of the M23 domain (CwIP-M23) and the SLT-peptidase M23 domain (CwIP-SLTM23), respectively (Fig. 1).

**Construction of Plasmid pQE-YomI-FL for Over-expression of Full Length of CwIP**—The region containing the full-length CwIP was PCR amplified using BF-YomI-FL and KR-YomI-FL primers, and *B. subtilis* 168 DNA. The amplified fragments were digested with *Bam*HI and *Kpn*I, and ligated to the corresponding sites in pQE-30, resulting in pQE-YomI-FL. The construct was used for over-expression of full-length CwIP (Fig. 1).

*Construction of Plasmids for*

*Over-expression of Mutated lines of CwlP-SLT and CwlP-M23*—To over-express various site-specific mutations within CwlP-SLT and CwlP-M23 proteins, new plasmids were created from pQE-SLT and pQE-M23, respectively. These were used as templates for site-directed mutagenesis using a QuikChange II kit (Stratagene), in accordance with the manufacturer's instructions. Amplification of the plasmids containing site-specific mutations was performed using two complementary DNA oligomers as primers (Supplemental Table S2). The plasmids, designated pQESLT-X (where X denotes any letter), were used to over-express the mutated versions of the CwlP-SLT proteins. These plasmids, pQEM23-X (where X denotes any letter), were used to over-express the mutated versions of the CwlP-M23 proteins. *E. coli* was transformed by plasmids as described by Sambrook *et al.* (6).

*Purification of Cell Wall and Peptidoglycan Components*—*B. subtilis* 168 cell wall and peptidoglycan components were prepared as described previously (7, 8, 9). *Staphylococcus aureus* and *Streptococcus thermophilus* cell walls and peptidoglycans were prepared in accordance with a method similar to that used for the preparation of *B. subtilis* cell walls and peptidoglycans.

*SDS-PAGE and Zymography*—SDS-PAGE and zymography were performed as described by Sambrook *et al.* (6) and Leclerc and Asselin (10), respectively. For zymography, renaturation of the proteins in SDS-gels were performed at 37°C or 40°C using a renaturation solution (1% Triton X-100, pH 5.0 or 7.5). The hydrolytic bands obtained from CwlP-SLT, CwlP-M23 and their mutated proteins were quantified using a CS analyzer equipped with 2.1 software (ATTO).

*Expression and Purification of Proteins*—CwlP-SLT, CwlP-M23, CwlP-SLTM23, full-length CwlP, and the mutated CwlP-SLT and CwlP-M23 proteins were over-expressed in *E. coli* JM109 harboring pQE-SLT, pQE-M23,

pQE-SLTM23, pQE-YomI-FL, pQESLT-X and pQEM23-X (where X denotes any letter), respectively. *E. coli* cells were incubated at 37°C in LB medium (containing 100 µg/ml ampicillin), in the presence or absence of 2% glucose. When the absorbance of the cultures reached 0.6-1.0 at 600 nm, 1 mM IPTG (final concentration) was added to the culture, and the cells incubated for a further 3 hours. Cells were harvested and suspended in 10 mM imidazole NPB buffer (10 mM imidazole, 1 M NaCl, 20 mM sodium phosphate, pH 7.4), and disrupted by sonication. After centrifugation a sample of the supernatant was used for purification of the proteins using a HiTrap Chelating HP column (GE Healthcare), in accordance with the manufacturer's instructions.

*Determination of the Hydrolytic Activities of the Recombinant Proteins for B. subtilis, S. aureus and S. thermophilus Cell Walls and Peptidoglycans and for E. coli Cells*—To identify the critical amino acid residues controlling the muramidase and D,D-endopeptidase activities of CwlP, we used 0.33 µM (5 µg/ml: final concentration) of the CwlP-SLT proteins, 0.15 µM (3 µg/ml: final concentration) of CwlP-M23 proteins, and 0.3 mg/ml of *B. subtilis* cell wall preparations. Comparison of the hydrolytic activities of the proteins were obtained by measurement of the cell wall densities using a spectrophotometer (V-560, JASCO), as described previously (11, 12). The hydrolytic reactions were performed in 50 mM MES-NaOH buffer (pH 5) at 37°C for CwlP-SLT and in 50 mM MOPS-NaOH buffer (pH 7.5) at 40°C for CwlP-M23.

To determine the hydrolytic activities of the proteins for the cell wall and peptidoglycan preparations, 0.1 µM of CwlP-SLT, CwlP-M23 and CwlP-SLTM23, and a mixture of 0.1 µM CwlP-SLT and 0.1 µM CwlP-M23 were used with 0.3 mg/ml *B. subtilis*, *S. aureus* and *S. thermophilus* cell walls or peptidoglycans. The hydrolytic reactions were performed at 40°C in 50 mM MOPS-NaOH buffer, pH 7.5 (for CwlP-M23); at 37°C in 50 mM MOPS-NaOH buffer, pH 7.5 (for CwlP-SLTM23 and the

mixture of CwIP-SLT and CwIP-M23); and at 37°C in 50 mM MES-NaOH buffer, pH 5 (for CwIP-SLT).

To measure the hydrolytic activity of the enzymes towards *E. coli* cells, 0.1 µM CwIP-SLT, CwIP-M23 or an aliquot of cells measuring 0.3 at OD<sub>600</sub> were used in reactions performed at 40°C in the presence of 50 mM MOPS-NaOH buffer, pH 7.5 (for CwIP-M23) and at 37°C in 50 mM MES-NaOH buffer, pH 5 (for CwIP-SLT).

*Determining the Effects of Divalent Cations on CwIP-M23 Activity*—Purified CwIP-M23 protein was dialyzed against 25 mM EDTA in 50 mM MOPS-NaOH (pH 7.5) to remove ions, and re-dialyzed against 50 mM MOPS-NaOH (pH 7.5). Purified cell walls were washed with a solution of 0.1 M EDTA followed by five washes with purified water. CwIP-M23 [0.077 µM (1.5 µg/ml): final concentration] was used to determine the effect of addition of 1 mM concentrations of various cations on hydrolytic activity. Reactions were performed at 40°C in 50 mM MOPS-NaOH buffer (pH 7.5).

*Preparation of N-acetylated Glycan Strands Containing GlcNAc-MurNAc Polymers*—Preparation of glycan strands (-[GlcNAc-MurNAc]<sub>n</sub>-) from *B. subtilis* peptidoglycans was performed as described previously (13). The prepared glycan strands were N-acetylated as described previously (13).

*CwIP-SLT Digestion of N-acetylated Glycan Strands*—One mg of the N-acetylated glycan strands were dissolved in 1 ml of 50 mM MES-NaOH buffer (pH 5.0), and 6.6 µM (0.1 mg/ml: final concentration) CwIP-SLT before incubation at 37°C for 12 hours. The solution was divided into two 0.5 ml aliquots prior to addition of phosphoric acid to one of them to change the pH to 2-3 (the “non-reduced sample”). 150 µl of 0.5 M borate buffer (pH 9.0) and 12.5 mg/ml (final concentration) of NaBH<sub>4</sub> was added to the other aliquot, which was incubated at 20°C for 30 min to reduce the oligosaccharides at the reducing ends, followed by adjustment of

the pH to 2-3 with phosphoric acid (the “reduced sample”).

*Separation of Glycan Strands Digested by CwIP-SLT* —“Non-reduced” and “reduced” digested samples were separated by RP-HPLC as described previously (13). A Symmetry Shield PR18 column (Waters), containing 0.05% TFA as elution buffer A, and 0.05% TFA containing 40% CH<sub>3</sub>CN, as elution buffer B was used for RP-HPLC. Elution was performed for 10 min with buffer A (non-gradient), then for 30 min using a linear gradient from 0 to 50% with buffer B.

*Determination of B. subtilis Peptidoglycan Cleavage Sites of CwIP-M23*—Purified peptidoglycan (0.3 mg/ml) was digested at 40°C in a pH 7.5 solution containing 0.77 µM (15 µg/ml: final concentration) CwIP-M23. Samples were collected at 0 and 30 min then boiled for at least 10 min. The 30 min-sample was divided into two. One half, the control sample, was incubated with 1 µM D,L-endopeptidase CwIE (LytF) (15 µg/ml: final concentration) (9) for 30 min then boiled for 10 min. All samples were treated with 7 µM lysozyme (0.1 mg/ml: final concentration) and incubated at 37°C overnight. Then after centrifugation, the supernatants were collected. 200 µl of the supernatants, 50 µl of 10% K<sub>2</sub>B<sub>4</sub>O<sub>7</sub>, and 250 µl of purified water were mixed together and 5 µl of 1 M 1-fluoro-2,4-dinitrobenzene (FDNB) was added to the samples. Labeling reactions of the free amino groups were performed using FDNB at 60°C for 30 min in the dark. 3 M HCl (final concentration) was added to the samples and kept at 95-100°C for 12 hours to digest the glycosidic and peptide bonds followed by neutralization with NaOH. The hydrolyzed samples were freeze-dried, and resuspended in 10% acetonitrile containing 0.025% trifluoroacetic acid (TFA). Samples were separated using RP-HPLC with a Wakosil-II 5C18 column (4.0 mm × 250 mm, Wako) (flow rate, 0.5 ml/min; detection wave length, 365 nm; column oven temperature, 40°C). The buffers used for elution were 0.025% TFA (buffer A) and 0.025% TFA containing 60% acetonitrile

(buffer B). Elution was performed for 60 min with a linear gradient between 0 to 100% in buffer B.

*Mass Spectrometry Determination of Separated Materials*—The RP-HPLC separated materials were freeze-dried and added to 50% CH<sub>3</sub>CN containing 0.05% TFA. Samples were identified by ESI-MS and ESI-MS/MS (Agilent 1100 series LC/MSD Trap VL).

## RESULTS

*The SLT and Peptidase M23 Domains of CwIP Exhibit Cell Wall Hydrolytic Activity*—CwIP (consisting of 2,285 amino acid residues) is related to the SP-beta prophage (2) and is the largest protein in the phage region. The Pfam database indicates that the protein appears to have at least three domains; an SLT domain (amino acids 1,424-1,534), a peptidase M23 domain (amino acids 1,578-1,674), and a phage-related minor tail protein (amino acids 387-587) (Fig. 1).

Based on the prediction that CwIP has two hydrolase domains, we used affinity chromatography to purify the CwIP-SLT and CwIP-M23 regions of this protein. Analysis of the SDS-gels from these experiments showed that the CwIP-SLT and CwIP-M23 domains were purified as single bands of the expected sizes (CwIP-SLT, 15.2 kDa; CwIP-M23, 19.6 kDa; Supplemental Fig. S1A and B). We used zymography to measure the hydrolytic activity of these domains because the strength of the hydrolytic bands in the gel depends on the enzymatic activity of the proteins (14). The zymography experiments showed that purified CwIP-SLT and CwIP-M23 both exhibited hydrolytic activity against *B. subtilis* cell walls (Supplemental Fig. S1A and B).

*The SLT domain of the Cell Wall Hydrolase CwIP, CwIP-SLT, has Muramidase Activity*—Because the SLT region of the CwIP protein appears to be a lytic transglycosylase that should be equipped to digest glycan strand linkages (between

MurNAc and GlcNAc), we tested the ability of CwIP-SLT to digest purified glycan strands derived from peptidoglycan of *B. subtilis*. The digested samples from this experiment were reduced then fractionated by RP-HPLC (Fig. 2A). Fig. 2A shows several peaks, indicating that CwIP-SLT can digest glycan strands. To determine the structure of the peak 2 material shown in Fig. 2A we used ESI-MS and ESI-MS/MS. This material produced fragment ions at  $m/z$  999.9 (positive mode) and 975.7 (negative mode) on ESI-MS, (Supplemental Fig. S2A and B); this corresponded to  $[M+Na]^+$  and  $[M-H]^-$  ions characteristic of a tetrasaccharide with a reduced end ( $M_r$  of reduced tetrasaccharide: 977). ESI-MS/MS analysis showed that because the ion series b<sub>2</sub>, b<sub>3</sub>, y<sub>2</sub> and y<sub>3</sub> in Fig. 3D were found among the fragment ions in Fig. 3A and B, the material from peak 2 could be identified as the tetrasaccharide, GlcNAc-MurNAc-GlcNAc-MurNAc. The structure of the peak 3 material observed in Fig. 2A was also determined using ESI-MS. In this case, the material in peak 3 gave a fragment ion at  $m/z$  1,454.9 (in the negative mode) (Supplemental Fig. S3A). This corresponded to the  $[M-H]^-$  ion of a hexasaccharide with a reduced end ( $M_r$  of reduced hexasaccharide: 1,456). Additional ESI-MS/MS analysis identified the peak 3 material as a hexasaccharide with a reduced end, namely, (GlcNAc-MurNAc)<sub>2</sub>-GlcNAc-MurNAc (Supplementary Fig. S3B and C). Therefore, CwIP-SLT is a muramidase that can digest MurNAc-GlcNAc linkages, but is not an *N*-acetylglucosaminidase.

To confirm that CwIP-SLT is a muramidase, purified glycan strands were digested with the enzyme and separated by RP-HPLC without reduction. As shown in Fig. 2B, the detected peaks produced were different from those observed in the reduced sample (Fig. 2A), indicating that the digested CwIP-SLT products had reducing ends. Furthermore, positive mode ESI-MS analysis of the peak B and C material produced fragment ions at  $m/z$  997.8 (data not shown) and 1,476.9 (data not shown), respectively. This result indicates that the peak B and C fragments correspond

to the  $[M+Na]^+$  ion of a tetrasaccharide ( $M_r$ , 975) and a hexasaccharide ( $M_r$ , 1,454), respectively. We also found that ESI-MS/MS analysis of the peak B material indicated that it was a tetrasaccharide containing a reducing end ( $[GlcNAc-MurNAc]_2$ ) (Fig. 3C and D). These results, therefore, strongly suggest that the SLT domain of CwIP exhibits only muramidase activity.

*Glu1447 is the Catalytic Amino Acid Residue within the Muramidase Domain of CwIP*—Our unexpected finding that the SLT domain of CwIP was, in fact, a muramidase (Figs. 2 and 3) motivated us to align the predicted domain sequence against other muramidase sequences from other bacterial species. Fig. 4A shows the alignment of the muramidase domain of CwIP and other proteins with high sequence similarity. Based on this alignment, conserved amino acid residues (except for hydrophobic and glycine residues) were selected for site-directed mutagenesis (black arrows in Fig. 4A).

The hydrolytic activities of all of the point-mutated proteins were measured by analyzing the turbidity of cell wall mixtures, as described in Experimental Procedures. Fig. 4B shows the relative hydrolytic activities of the mutated proteins compared with the activity of the wild-type protein. We found that mutating residue Glu1447 to either E1447Q or E1447A, abolished all enzyme activity. However, all seven of the other mutated CwIP-SLT domains exhibited some degree of muramidase activity, in comparison with the wild-type (Fig. 4B).

It is possible that some of the mutated proteins may have had decreased hydrolytic activities due to misfolding or conformation changes in the protein. Zymography is a technique that some of renatured proteins in a gel can assume an active form (14). Thus, only mutations that result in completely inactive proteins can be identified with this technique. The mutated CwIP proteins, E1447Q and E1447A, exhibited no activity in the zymography experiments [Relative activities of E1447Q and E1447A compared with wild-type CwIP-SLT were 0.7 % and 1.1 %, respectively (Supplemental Table S3)].

However, because the other mutations exhibited some muramidase activity (Supplemental Table S3), these results provide strong evidence that Glu1447 is indeed the critical amino acid residue controlling muramidase activity.

*Peptidoglycan Cleavage Sites of CwIP-M23 in B. subtilis*—Because the zymography experiments showed that the peptidase M23 domain of CwIP exhibited cell wall hydrolytic activity toward *B. subtilis* cell walls (Supplemental Fig. S1B), we sought to determine the CwIP-M23 cleavage site within *B. subtilis* peptidoglycan preparations. Purified *B. subtilis* peptidoglycan was digested by CwIP-M23 and free amino groups of the digested peptidoglycan were labeled with FDNB, followed by digestion of the peptide and glycoside bonds with HCl (see Experimental Procedures). The sample (containing DNP-amino acids), was separated by RP-HPLC. As shown in Fig. 5B, only the peak 1 material identified as a mono-DNP- $A_2pm$  using mass spectrometry (data not shown) was drastically increased in the sample. The result indicates that the enzyme is a D,D-endopeptidase that produced only one free amino group in  $A_2pm$ .

To confirm CwIP-M23 is not a D, L-endopeptidase that produces two free amino groups in  $A_2pm$ , the CwIP-M23 digested peptidoglycan was further digested with LytF (CwIE), (a D, L-endopeptidase) (9). Because the CwIP-M23 and LytF digested peptidoglycan sample contained bis-DNP- $A_2pm$  (Supplemental Fig. S4), it was found that CwIP-M23 was only able to digest the cross-linkage between D-alanine and  $A_2pm$ , which is a characteristic of the activity of a D, D-endopeptidase.

*His1628 and His1660 are Essential Amino Acid Residues for the D,D-endopeptidase Activity of CwIP*—The peptidase M23 domain cleaves the cross-linkage between D-alanine and  $A_2pm$ , but it is known that this domain also digests linkages between Gly-Gly or L-Ala-D-Glu in peptidoglycan molecules (4, 5). To investigate the digestion pattern of CwIP, the peptidase M23 domain of

this protein was aligned against similar proteins from other bacteria. Based on the sequence alignments shown in Fig. 6A, conserved amino acid residues (except for hydrophobic amino acids and glycine residues) were selected for analysis using site-directed mutagenesis. The selected amino acid residues were point-mutated, and the hydrolytic activities against *B. subtilis* cell walls were determined by measuring the reduction in turbidity of cell wall preparations. As shown in Fig. 6B, only H1628Q and H1660Q exhibited no enzymatic activity. Of the other eight mutated CwIP-M23 proteins, all exhibited activity >5% of the wild-type enzyme (Fig. 6B).

To verify that H1628Q and H1660Q had no hydrolase activity, zymography was performed using both CwIP-M23 and the mutated proteins. The mutated proteins, H1580Q, D1584N and H1662Q, exhibited very weak activities (relative activities compared with the wild-type CwIP-M23 enzyme were 6.1 %, 5.6 % and 8.9 %, respectively (Supplemental Table S3). However, we found that H1628Q and H1660Q exhibited no activity (relative activities compared with wild-type CwIP-M23 are 0.2 % and 1.5 %, respectively (Supplemental Table S3). Therefore, these results suggest that His1628 and His1660 are essential amino acid residues for D,D-endopeptidase activity.

*Hydrolytic Activities and Divalent Cation requirements of CwIP-SLT and CwIP-M23 towards B. subtilis Cell Walls*—Because our experiments showed that CwIP-SLT and CwIP-M23 were both novel hydrolases, the effects of divalent cations on their activities were investigated. We found that the muramidase activity of CwIP-SLT was unaffected by the presence of several different divalent cations, or when cation-free conditions were used (data not shown). The D,D-endopeptidase, CwIP-M23, however, exhibited stronger activity in the presence of  $\text{Ca}^{2+}$  and  $\text{Co}^{2+}$ , but no activity was observed when  $\text{Zn}^{2+}$  and  $\text{Mg}^{2+}$  were present in the reactions (Fig. 6C).

*Species Specific Hydrolytic Activity of CwIP for Cell Walls and Peptidoglycans*—CwIP is a SP-beta prophage protein, therefore, it may be possible that it can digest not only *B. subtilis* cell walls but other bacterial cell walls as well. We investigated the enzyme activity of CwIP against purified cell walls obtained from other bacterial species including, *S. aureus* (-GlcNAc-MurNAc[-L-Ala-D-Gln-L-Lys-D-Ala]<sub>n</sub> cross-linked between D-Ala and L-Lys with Gly<sub>5</sub> (15) and *S. thermophilus* (-GlcNAc-MurNAc[-L-Ala-D-Glu-L-Lys-D-Ala]<sub>n</sub> cross-linked between D-Ala and L-Lys with L-Ala<sub>2</sub> (16), using hydrolysis assays.

To determine the hydrolytic activity of CwIP, the protein designated CwIP-SLTM23 (which contains a muramidase domain and a D,D-endopeptidase domain), together with the full-length CwIP were over-expressed in *E. coli*. Purified CwIP-SLTM23 protein preparations exhibited hydrolytic activity against *B. subtilis* cell walls, as determined by zymography (Supplemental Fig. S1C). However, the full-length version of CwIP was not able to digest cell walls, as observed by zymography (Supplemental Fig. S1D). This could be because the full-length CwIP may be an inactive precursor, or may not have been renatured to an active form under the renaturation conditions used to digest *B. subtilis* cell walls or because of its large size, which is > 200 kDa. CwIP-SLT, CwIP-M23 and CwIP-SLTM23 enzymes were also used to determine hydrolytic activity. As shown in Fig. 7A, all of these enzymes were able to digest *B. subtilis* cell walls, but none could digest the cell walls of *S. aureus* and *S. thermophilus* (Fig. 7C, D, and data not shown).

CwIP-M23 exhibited much stronger activity under optimum conditions for enzyme activity (i.e. 1 mM  $\text{CaCl}_2$ , Fig. 6C) using *B. subtilis* cell walls. Thus, the hydrolytic activities of CwIP-M23 and CwIP-SLTM23 toward *S. aureus* and *S. thermophilus* cell walls were determined using 1 mM  $\text{CaCl}_2$ . However, no activities were detected using such conditions (data not shown). Our results, therefore, indicate that CwIP may only be able to digest *B. subtilis*

cell walls. *S. aureus* and *S. thermophilus* cell walls, used as positive controls in this experiment, could be efficiently digested by D, L-endopeptidase (*B. subtilis* LytF) and lysozyme (data not shown).

It is known that the cells walls from Gram-positive bacteria contain peptidoglycan and anion polymers such as teichoic acids and teichuronic acids (17). We investigated if the peptidoglycan polymers of *B. subtilis*, *S. aureus* and *S. thermophilus* could be digested by CwIP enzymes (following removal of anion polymers from the preparations). As shown in Fig. 7B, C and D, CwIP-SLT could digest peptidoglycans derived from all three species of bacteria. Moreover, CwIP-SLT could also digest *E. coli* cells (Supplemental Fig. S5). This may be because *E. coli* does not contain anion polymers in its cell walls and the peptidoglycan structure is identical to *B. subtilis* (18). In contrast, CwIP-M23 was only able to digest *B. subtilis* peptidoglycan and *E. coli* cells (Fig. 7B, C, and D, and Supplemental Fig. S5). These results indicate, therefore, that CwIP may hydrolyze cell walls similar to that of *B. subtilis*.

## DISCUSSION

In this study, we demonstrated that CwIP has muramidase activity but lacks lytic transglycosylase activity. The critical amino acid residue controlling the muramidase activity of the enzyme was found to be Glu1447 (Fig. 4B and Supplemental Table S3). We previously reported that the N-terminal domain of CwlT exhibits muramidase activity, and that the critical amino acid residues comprised Glu87 and Asp94 (Fig. 4A) (19). In that report, we hypothesized that Glu87 was the critical amino acid residue controlling hydrolytic activity, because other muramidases such as HEWL (20,21), T4L (22), and GEWL (23), have a conserved glutamic acid residue in the corresponding position that controls their catalytic activity. Because the glutamic acid residue is conserved in all muramidases characterized to date, including CwIP and lytic transglycosylases (such as Slt70), it appears likely that it could be involved in the

hydrolytic activity of the enzyme. Nevertheless, Asp94 of CwlT also appears to be associated with hydrolytic activity, either directly or indirectly (19). However, Weaver *et al.* reported that GEWL lacks a catalytic aspartic acid residue on the basis of their crystallographic analysis of the protein (24). Supporting this finding, inspection of the muramidase domain of CwIP shows that it has no candidate catalytic aspartic acid residue within its sequence (Fig. 4A). Therefore, it is possible that the aspartic acid residue found in a few characterized muramidases is not directly involved in hydrolysis of the glycosidic linkage of MurNAc-GlcNAc.

The M23 domain of CwIP was able to digest linkages between D-Ala and A<sub>2</sub>pm, which comprise the cross-linked peptide side chains of the *B. subtilis* peptidoglycan (Fig. 5). It is known that the M23 family includes the Gly-Gly endopeptidases of the lysostaphin type (25) such as that found in *S. aureus* LytM and *Staphylococcus capitis* Ale1 (4, 26). Very few enzymes within the metalloendopeptidase family (e.g. gp13 in the  $\phi$ 29 *Bacillus* bacteriophage), can digest D-Ala-A<sub>2</sub>pm linkages. However, no linkage digesting enzymes have been identified in “the M23 endopeptidase family”, as predicted from inspection of the Pfam database. Interestingly, CwIP-M23 exhibited no significant activity toward *S. aureus* or *S. thermophilus* cell wall or peptidoglycan preparations (Fig. 7C, D and data not shown). Therefore, we conclude that CwIP-M23 cannot digest Gly-Gly and Ala-Ala linkages, and appears to specifically act as a D-alanyl-A<sub>2</sub>pm endopeptidase.

We also found that the critical amino acid residues within CwIP-M23 were His1628 and His1660, because in our experiments, the mutated CwIP, H1628Q and H1660Q proteins exhibited no hydrolytic activity (Fig. 6B and Supplemental Table S3). The position of the conserved histidine residue (His1660) of CwIP is His291 in *S. aureus* LytM and His231 in *S. capitis* Ale1; both of these positions have been identified as catalytic residues (27, 28). With regard to His1628 of CwIP, this conserved residue corresponds to

His260 of LytM and His200 of Ale1. Fujiwara *et al.* reported that His200 in Ale1 lies within one of the active sites (27), and Odintsov *et al.* indicated that His-260 in LytM was a candidate catalytic amino acid residue (28). Hence, it appears likely that both histidine residues within CwIP-M23, LytM and Ale1 are necessary for their endopeptidase activities.

It is noteworthy that the other CwIP-M23 mutants, H1580Q, D1584N and H1662Q, exhibited small amounts of hydrolytic activity (Fig. 6B and Supplemental Table S3). The above three residues are also conserved in LytM and Ale1 where they appear to be metal binding sites (arrowheads in Fig. 6A) (27, 29). Because CwIP-M23 needs divalent cations such as  $\text{Ca}^{2+}$ ,  $\text{Co}^{2+}$  and  $\text{Mn}^{2+}$  for its catalytic activity (Fig. 6C), it is predicted that His1580, Asp1584 and His1662 of CwIP are metal binding sites. Interestingly  $\text{Zn}^{2+}$  appears not to be an optimum divalent cation for CwIP-M23 activity (Fig. 6C), despite the fact that LytM and Ale1 are both  $\text{Zn}^{2+}$ -dependent metalloendopeptidases (26, 30).  $\phi 29$  *Bacillus* bacteriophage gp13 (D-alanyl- $\text{A}_2\text{pm}$  endopeptidase) also requires a  $\text{Zn}^{2+}$  ion for activity (31). We conclude, therefore, that the CwIP-M23 enzyme is unique because it does not depend on  $\text{Zn}^{2+}$  for catalytic activity.

CwIP is a phage-related protein whose coding sequence is located in the SP-beta prophage (2). At 2,285 amino acids in length, or 252 kDa, CwIP is the largest protein in the prophage region. Because CwIP has a phage-related minor tail domain, it is possible that it functions as a tail protein. Recently, Piuri and Hatfull described the gp17 of the tape measure protein (*Tmp*), as a mycobacteriophage tail protein (1). The 1,229 amino acid *Tmp* protein contains a cell wall hydrolase that facilitates efficient infection of stationary phase cells (1). Interestingly, Kenny *et al.* showed that Orf50 of the bacteriophage Tuc2009 (906 a.a.) encodes a tail-associated cell wall-degrading activity that mediates infection through cell wall hydrolysis (32). However, it is not known whether CwIP functions as a tail protein. Further studies of CwIP function in infection with the point-mutated *cwIP* and null-mutated

*cwIP* *in vivo* are ongoing in our laboratory.

CwIP-SLT, CwIP-M23 and CwIP-SLTM23 showed no significant hydrolytic activity toward *S. aureus* and *S. thermophilus* cell walls (Fig. 7C, D and data not shown). Because the peptidase M23 domain of CwIP is a D-alanyl- $\text{A}_2\text{pm}$  peptidase, the enzyme should be able to digest target linkages accurately, resulting in no digestion of either cell wall or peptidoglycan. Although the muramidase domain of CwIP appears to be able to digest the glycan strands of various peptidoglycans, it was not able to digest *S. aureus* and *S. thermophilus* cell walls (Fig. 7C, D and data not shown). It is possible that modifications in these cell walls, such as the presence of anion polymers, may inhibit the hydrolytic activity of the muramidase domain of CwIP. In fact, our studies showed that the CwIP muramidase domain could digest *B. subtilis*, *S. aureus* and *S. thermophilus* peptidoglycans, and *E. coli* cell walls, which have no anion polymers (Fig. 7B, C, D, and Supplemental Fig. S5). Consequently, the muramidase domain of CwIP appears to have a restricted hydrolase activity against cell walls.

The full-length CwIP amino acid sequence is conserved in *B. subtilis*. *S. aureus* phage proteins (such as Q6GAK2\_STAAS and Q8SDP3\_9CAUD) are unique in having a three domain structure, which includes a phage-related minor tail protein, a peptidase M23 domain, and a SLT domain. Their sizes are similar to the CwIP protein (>2,000 a.a.); however, outside the three domain regions, their sequences are quite dissimilar to CwIP. Accordingly, the SP-beta phage (containing CwIP) can only infect *B. subtilis* cells, because digestion with CwIP-SLTM23 is restricted to *B. subtilis* cell walls.

This is the first study of a newly categorized muramidase domain that has striking similarities with the *E. coli* Slt70 protein, both in the amino acid sequence and its catalytic residues. The fact that the peptidase M23 domain of CwIP is a unique  $\text{Zn}^{2+}$ -independent D-alanyl- $\text{A}_2\text{pm}$  endopeptidase, means it was unlikely to have been included in the peptidase M23 family in the Pfam database.

*Acknowledgments*—We thank Dr. K. Ozaki (Kao Corp., Tochigi, Japan) for preparing the *B. subtilis* 168 cells to obtain cell walls, Dr. K. Oana (School of Medicine, Shinshu University, Japan) for the gift of several Gram-positive bacterial cells, and Dr. H. Karasawa (Nagano Prefecture General Technology Center, Nagano, Japan) for helping molecular weight determination using ESI-MS and ESI-MS/MS. We also thank Dr. T. Kodama and Ms. K. Kobayashi for helpful discussion and Ms. K. Takahashi (Division of Gene Research) for editing this manuscript.

## REFERENCES

1. Piuri, M., and Hatfull, G. F. (2006) *Mol. Microbiol.* **62**, 1569-1585
2. Kunst, F., *et al.* (1997) *Nature* **390**, 249-256
3. Regamey, A., and Karamata, D. (1998) *Microbiology* **144**, 885-893
4. Ramadurai, L., Lockwood, K. J., Nadakavukaren, M. J., and Jayaswal, R. K. (1999) *Microbiology* **145**, 801-808
5. Horsburgh, G. J., Atrih, A., and Foster, S. J. (2003) *J. Bacteriol.* **185**, 3813-3820
6. Sambrook, J., Fritsch, E. F., and Maniatis, T. (1989) *Molecular Cloning: A Laboratory Manual*, 2nd Ed., Cold Spring Harbor Laboratory Press, Cold Spring Harbor, N.Y
7. DeHart, H. P., Heath, H. E., Heath, L. S., LeBlanc, P. A., and Sloan, G. L. (1995) *Appl. Environ. Microbiol.* **61**, 1475-1479
8. Fein, J. E., and Rogers, H. J. (1976) *J. Bacteriol.* **127**, 1427-1442
9. Ohnishi, R., Ishikawa, S., and Sekiguchi, J. (1999) *J. Bacteriol.* **181**, 3178-3184
10. Leclerc, D., and Asselin, A. (1989) *Can. J. Microbiol.* **35**, 749-753
11. Fukushima, T., Afkham, A., Kurosawa, S., Tanabe, T., Yamamoto, H., and Sekiguchi, J. (2006) *J. Bacteriol.* **188**, 5541-5550
12. Fukushima, T., Yao, Y., Kitajima, T., Yamamoto, H., and Sekiguchi, J. (2007) *Mol. Genet. Genomics.* **278**, 371-383
13. Fukushima, T., Kitajima, T., and Sekiguchi, J. (2005) *J. Bacteriol.* **187**, 1287-1292
14. Shida, T., Hattori, H., Ise, F., and Sekiguchi, J. (2001) *J. Biol. Chem.* **276**, 28140-28146
15. Tong, G., Pan, Y., Dong, H., Pryor, R., Wilson, G. E., and Schaefer, J. (1997) *Biochemistry* **36**, 9859-9866
16. Layec, S., Gérard, J., Legué, V., Chapot-Chartier, M. P., Courtin, P., Borges, F., Decaris, B., and Leblond-Bourget, N. (2009) *Mol. Microbiol.* **71**, 1205-1217
17. Foster, S. J., and Popham, D. L. (2002) *Bacillus subtilis and Its Closest Relatives: From Genes to Cells* (Sonenshein, A. L., Hoch, J. A., and Losick, R., eds) pp. 21-41, American Society for Microbiology, Washington, D.C.
18. Park, J. T., and Uehara, T. (2008) *Microbiol. Mol. Biol. Rev.* **72**, 211-227
19. Fukushima, T., Kitajima, T., Yamaguchi, H., Ouyang, Q., Furuhashi, K., Yamamoto, H., Shida, T., and Sekiguchi, J. (2008) *J. Biol. Chem.* **283**, 11117-11125
20. Malcolm, B. A., Rosenberg, S., Corey, M. J., Allen, J. S., de Baetselier, A., and Kirsch, J. F. (1989) *Proc. Natl. Acad. Sci. U. S. A.* **86**, 133-137
21. Matsumura, I., and Kirsch, J. F. (1996) *Biochemistry* **35**, 1881-1889
22. Kuroki, R., Weaver, L. H., and Matthews, B. W. (1999) *Proc. Natl. Acad. Sci. U. S. A.* **96**, 8949-8954
23. Thunnissen, A. M., Rozeboom, H. J., Kalk, K. H., and Dijkstra, B. W. (1995) *Biochemistry* **34**, 12729-12737
24. Weaver, L. H., Grütter, M. G., and Matthews, B. W. (1995) *J. Mol. Biol.* **245**, 54-68
25. Kumar, J. K. (2008) *Appl. Microbiol. Biotechnol.* **80**, 555-561
26. Sugai, M., Fujiwara, T., Akiyama, T., Ohara, M., Komatsuzawa, H., Inoue, S., and Suginaka, H. (1997) *J. Bacteriol.* **179**, 1193-1202
27. Fujiwara, T., Aoki, S., Komatsuzawa, H., Nishida, T., Ohara, M., Suginaka, H., and Sugai,

- M. (2005) *J. Bacteriol.* **187**, 480-487
28. Odintsov, S. G., Sabala, I., Marcyjaniak, M., and Bochtler, M. (2004) *J. Mol. Biol.* **335**, 775-785
29. Bochtler, M., Odintsov, S. G., Marcyjaniak, M., and Sabala, I. (2004) *Protein. Sci.* **13**, 854-861
30. Firczuk, M., Mucha, A., and Bochtler, M. (2005) *J. Mol. Biol.* **354**, 578-590
31. Cohen, D. N., Sham, Y. Y., Haugstad, G. D., Xiang, Y., Rossmann, M. G., Anderson, D. L., and Popham, D. L. (2009) *J. Mol. Biol.* **387**, 607-618
32. Kenny, J. G., McGrath, S., Fitzgerald, G. F., and van Sinderen, D. (2004) *J. Bacteriol.* **186**, 3480-3491
33. Grütter, M. G., Weaver, L. H., and Matthews, B. W. (1983) *Nature* **303**, 828-831
34. Thunnissen, A. M., Isaacs, N. W., and Dijkstra, B. W. (1995) *Proteins* **22**, 245-258
35. Hirakawa, H., Ochi, A., Kawahara, Y., Kawamura, S., Torikata, T., and Kuhara, S. (2008) *J. Biochem.* **144**, 753-761
36. van Asselt, E. J., Thunnissen, A. M., and Dijkstra, B. W. (1999) *J. Mol. Biol.* **291**, 877-898

#### FOOTNOTES

\* This work was supported by Grants-in-Aid for Scientific Research (B) (19380047) and (A) (22248008), and by the New Energy and Industrial Technology Department Organization (NEDO) to J. S; by a Grant-in-Aid for Young Scientists (21780067) to T. F; and by the Global COE programs (to J. S., T. F., and I. P. S) of the Ministry of Education, Culture, Sports, Science, and Technology of Japan.

This paper is dedicated to the first principal, Chotaro Harizuka, on the occasion of the 100th anniversary of the Faculty of Textile Science and Technology, Shinshu University.

<sup>s</sup> The on-line version of this article (available at <http://www.jbc.org>) contains Supplemental Tables S1-S3 and Figures. S1-S5.

<sup>3</sup> Abbreviations: PCR, polymerase chain reaction; SDS, sodium dodecyl sulfate; PAGE, polyacrylamide gel electrophoresis; RP-HPLC, reverse phase-high performance liquid chromatography; aa, amino acid(s); DNP, dinitrophenyl; A<sub>2</sub>pm, diaminopimelic acid; FDNB, 1-fluoro-2,4-dinitrobenzene; IPTG, isopropyl beta-D-thiogalactopyranoside; GlcNAc, N-acetylglucosamine; MurNAc, N-acetylmuramic acid; MurNAcr, MurNAc with a reduced end; ESI-MS, electrospray ionization-mass spectrometry; TFA, trifluoroacetic acid; SLT, soluble lytic transglycosylase; GEWL, goose egg-white lysozyme; HEWL, hen egg-white lysozyme; T4L, bacteriophage T4 lysozyme.

## FIGURE LEGENDS

**FIGURE 1. Open reading frames around the *cwIP* region and domain structure of CwIP.** The *cwIP* gene is located between the *yomK-yomJ* operon and *yomH-yomG* operon in the SP-beta region (2). *yomK*, *yomJ*, *yomH* and *yomG* genes are function unknown. CwIP consists of 2,285 amino acids residues, and at least three domains have been classified in the Pfam database. These include a phage-related minor tail protein (shadow box), an SLT domain (black box, which is actually a muramidase domain), and a peptidase M23 domain (dark gray box, D,D-endopeptidase domain). Numbers indicate the positions of amino acid residues from the first amino acid, Met, of CwIP. The purified proteins, CwIP-SLT, CwIP-M23, CwIP-SLTM23 and full-length CwIP, were shown to have these domain structures.

**FIGURE 2. RP-HPLC analysis of glycan strands digested with CwIP-SLT.** After purified glycan strands from *B. subtilis* peptidoglycan had been digested with CwIP-SLT, the reducing end of the amino sugar groups were reduced (panel A, “reduced sample”) or left untreated (panel B, “non-reduced sample”), then separated by RP-HPLC as described in “Experimental Procedures”. The numbers on the peaks indicate retention times. The materials from peaks 1, 2 and 3 in panel A were identified as GlcNAc-MurNAc (peak 1, data not shown), GlcNAc-MurNAc-GlcNAc-MurNAc (peak 2, Fig. 3A, B, D and Supplemental Fig. S2A and B), and (GlcNAc-MurNAc)<sub>2</sub>-GlcNAc-MurNAc (peak 3, Supplemental Fig. S3). The materials from peaks B and C in panel B were identified as (GlcNAc-MurNAc)<sub>2</sub> (peak B, Fig. 3C and D) and (GlcNAc-MurNAc)<sub>3</sub> (peak C, data not shown). When the glycan strands were digested with the enzyme for a longer time followed by reduction, only peaks 1 and 2 were observed (data not shown).

**FIGURE 3. ESI-MS/MS analysis of the peak 2 material in Fig. 2A and peak B material in Fig. 2B.** Panels A and B show the results for the peak 2 material (a reduced tetrasaccharide) from MS/MS analysis conducted in positive and negative modes, respectively. The precursor ions obtained using both modes were [M+Na]<sup>+</sup> (*m/z* 999.9) and [M-H]<sup>-</sup> (*m/z* 975.6), thus the material in peak 2 was identified as GlcNAc-MurNAc-GlcNAc-MurNAc. Panel C: the results for the peak B material (a non-reduced tetrasaccharide) from MS/MS analysis performed in the positive mode. The precursor ion obtained was [M+Na]<sup>+</sup> (*m/z* 997.8), and the material in peak B was identified as GlcNAc-MurNAc-GlcNAc-MurNAc. Panel D: the structure identified and the calculated molecular weight of each fragment in peaks 2 and B. For the peak B material, the structure identified was similar to the peak 2 structure. However, the MurNAc structure (gray broken box; peak 2) is different from MurNAc (black broken box; peak B). Ion series *b* and *y*, and *b'* and *y'* correspond to the fragment peaks of the materials in peak 2 (GlcNAc-MurNAc-GlcNAc-MurNAc) and peak B (GlcNAc-MurNAc-GlcNAc-MurNAc), respectively.

**FIGURE 4. Identification of the critical amino acid residues involved in CwIP muramidase activity.** (A) Alignment of the muramidase domain of CwIP, homologous proteins, lytic transglycosylases, and muramidases. The alignment was performed using the Pfam database. The characterized or predicted critical amino acid residues for the hydrolytic activity (references 19, 33, 34, 35) are shown in boxes. Amino acid residues identical to those in the CwIP sequence are shaded. Numbers indicate the amino acid positions from the N-terminus. Gray rectangles and broken arrows denote secondary structures,  $\alpha$ -helices and  $\beta$ -sheets in the Slr70 *E. coli* protein (SLT\_ECOLI) (23, 36). Arrows indicate amino acid residues that were mutated. An asterisk denotes the amino acid that was exchanged and is not conserved between SLT\_ECOLI and MltC\_ECOLI. Abbreviations: CwIP\_SLT, SLT domain (exhibiting CwIP muramidase activity); YjbJ\_BACSU, *Bacillus subtilis* YjbJ protein; YjbJ\_BACLI, *B. licheniformis* YjbJ

protein; YjbJ\_BACHA, *B. halodurans* YjbJ protein; Geobacillus, *Geobacillus* sp. protein; Heliobacterium, *Heliobacterium modesticaldum* protein; Shewanella, *Shewanella benthica* protein; Acinetobacter, *Acinetobacter baumannii* protein; Lawsonia, *Lawsonia intracellularis* protein; Pelotomaculum, *Pelotomaculum thermopropionicum* protein; Lysinibacillus, *Lysinibacillus sphaericus* protein; Oceanobacillus, *Oceanobacillus iheyensis* protein; Clostridium, *Clostridium cellulolyticum* protein; Desulfotomaculum, *Desulfotomaculum reducens* protein; SLT\_ECOLI, soluble lytic transglycosylase 70 in *E. coli*; MltC\_ECOLI, membrane-bound lytic murein transglycosylase C in *E. coli*; LYG\_ANSAN, *Anser anser anser* goose-type lysozyme; CwIT\_N, N-terminal domain (muramidase) of CwIT. Panel B: *In vitro* cell wall hydrolytic activity. Purified cell walls (0.3 mg/ml) were digested with 1  $\mu$ M (15  $\mu$ g/ml) CwIP-SLT or the mutated CwIP-SLT for 30 min at 37°C (pH 5.0). The reduction in the turbidity of the solution for the mutated CwIP-SLT was compared with that of the wild-type CwIP-SLT. In this experiment, the mutated residues E1447Q and E1447A exhibited no activity toward *B. subtilis* cell walls.

**FIGURE 5. Determination of CwIP-M23 cleavage sites using RP-HPLC.** *B. subtilis* peptidoglycan (containing no anionic polymers) was cleaved without (panel A) or with (panel B) CwIP-M23 for 30 min. The free amino acid residues in the samples were labeled with FDNB and the samples were hydrolyzed with HCl. Samples were separated by RP-HPLC. Both samples contained only the material derived from peak 1 (mono-DNP-A<sub>2</sub>pm) or peak 2 (DNP). An arrow indicates the (54 min) retention time of bis-DNP-A<sub>2</sub>pm. The peptidoglycan sample digested with CwIP-M23 and LytF (D,L-endopeptidase) gave three peaks; peaks 1 and 2, and a new peak derived from bis-DNP-A<sub>2</sub>pm that had a 54 min retention time on RP-HPLC (Supplemental Fig. S4).

**FIGURE 6. Identification of the CwIP catalytic amino acid residues controlling D,D-endopeptidase activity (digestion of linkage between D-Ala and A<sub>2</sub>pm) and the effect of divalent cations.** (A) Alignment of the M23 domain of CwIP, homologous proteins, and Gly-Gly, L-Ala-D-Glu and D-Ala-A<sub>2</sub>pm endopeptidases. The protein sequences were aligned using the ClustalW algorithm (see <http://align.genome.jp/>). The hydrolytic amino acid residues that are not related to the metal binding are denoted by boxes. Zinc binding sites in *S. aureus* LytM (28), *S. capitis* Ale1 (27), or  $\phi$ 29 *Bacillus* bacteriophage gp13 (31) are denoted by arrowheads (the open arrowhead shows the Zn<sup>2+</sup> binding site for LytM and Ale1, and the closed arrowheads represent Zn<sup>2+</sup> binding sites for LytM, Ale1 and gp13), respectively. Residues that are identical to CwIP are represented by shading, and the numbers represent amino acid positions starting from the N-terminus of each protein. The gray rectangle and arrows represent  $\alpha$ -helix and  $\beta$ -sheets, respectively, in *S. aureus* LytM (28). The HXH motif is the consensus one for Zn<sup>2+</sup>-metallopeptidases (28) and is conserved in all of the proteins shown here. However, the Asp-His motif described by Bochtler *et al.* differs between gp13 and many other proteins (HX<sub>6</sub>D and HX<sub>3</sub>D, respectively) (where X is any letter) (29). Arrows indicate amino acid residues that were mutated in this study. Asterisks denote the critical amino acid residues within CwIP-M23 that were identified in this study. Abbreviations: CwIP-M23, *B. subtilis* CwIP; Clostridium, *Clostridium nexile* protein; Ruminococcus, *Ruminococcus lactaris* protein; Dorea, *Dorea formicigenerans* protein; Eubacterium, *Eubacterium ventriosum* protein; Roseburia, *Roseburia intestinalis* protein; Bacteroides, *Bacteroides capillosus* protein; Lawsonia, *Lawsonia intracellularis* protein; Vibrio, *Vibrio alginolyticus* protein; Streptomyces, *Streptomyces clavuligerus* protein; LytM\_STAA8, *S. aureus* LytM; Ale1\_STACP, *Staphylococcus capitis* Ale1; LytH\_BACSU, *B. subtilis* LytH; Phi29 gp13,  $\phi$ 29 *Bacillus* bacteriophage gp13. *S. aureus* LytM and *S. capitis* Ale1 are Gly-Gly endopeptidases (4, 26). *B. subtilis* LytH is an L-Ala-D-Glu endopeptidase (5).  $\phi$ 29 *Bacillus* bacteriophage gp13 is a D-Ala-A<sub>2</sub>pm endopeptidase (31). (B) *In vitro* cell wall hydrolytic activity. Purified cell walls (0.3 mg/ml) were digested with 0.15  $\mu$ M (3

µg/ml) CwIP-M23 or the mutated CwIP-M23 for 30 min at 40°C (pH 7.5). The reduction in turbidity of the solution was measured, and the decrease in turbidity with the mutated CwIP-M23 was compared with that of the wild-type, CwIP-M23. In this experiment, H1628Q and H1660Q exhibited no hydrolytic activity. (C) Hydrolytic activity of CwIP-M23 in the presence of divalent cations. After purified CwIP-M23 had been dialyzed against 25 mM EDTA and re-dialyzed against 50 mM MOPS-NaOH (pH 7.5), the turbidity of a cell wall solution (0.3 mg/ml) with 0.077 µM (1.5 µg/ml) CwIP-M23 and various divalent cations (1 mM) was measured (at 40°C, pH 7.5). Closed squares: intact CwIP-M23 (without dialysis against EDTA); closed circles, Ca<sup>2+</sup> ion; closed diamonds, Co<sup>2+</sup> ion; closed triangles, Mn<sup>2+</sup> ion; open squares, no cation; open circles, Zn<sup>2+</sup> ion; open diamonds, Ni<sup>2+</sup> ion; open triangles, Mg<sup>2+</sup> ion. Error bars in panel C indicate the standard deviations for three independent experiments.

**FIGURE 7. Hydrolytic activity toward cell wall and peptidoglycan preparations.** (A) and (B) Hydrolytic activity toward *B. subtilis* cell wall (panel A) and peptidoglycan (panel B). (C) Hydrolytic activity toward *S. aureus* cell wall and peptidoglycan preparations. (D) Hydrolytic activity toward *S. thermophilus* cell wall and peptidoglycan. The hydrolytic activity of CwIP-SLTM23 toward *S. aureus* and *S. thermophilus* cell walls is shown in panels C and D, respectively. Open circles, no enzyme (panel A) or CwIP-SLTM23 cell wall directed activity (panels C and D); closed squares, CwIP-SLT activity towards cell walls (panel A) and peptidoglycans (panels B, C and D); closed triangles, CwIP-M23 activity towards cell walls (panel A) and peptidoglycans (panels B, C and D); closed circles, CwIP-SLTM23 activity toward cell walls (panel A) and peptidoglycans (panels B, C and D); closed diamonds, mixture of CwIP-SLT and CwIP-M23 activities towards cell walls (panel A) and peptidoglycans (panels B, C and D). CwIP-SLT, CwIP-M23 and mixtures of CwIP-SLT and CwIP-M23 exhibited no activity toward *S. aureus* and *S. thermophilus* cell walls, in common with CwIP-SLTM23 (open circles in panels C and D). The error bars indicate the standard deviations from three independent experiments.

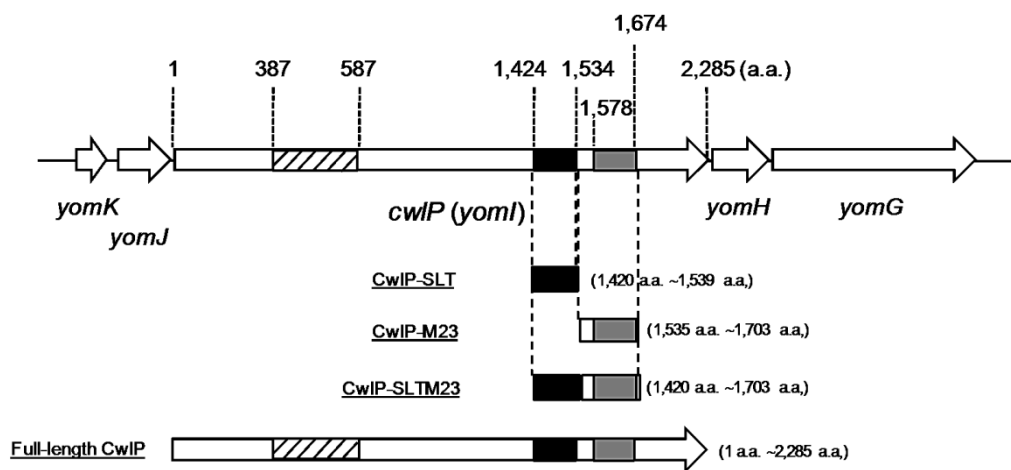


FIGURE. 1.

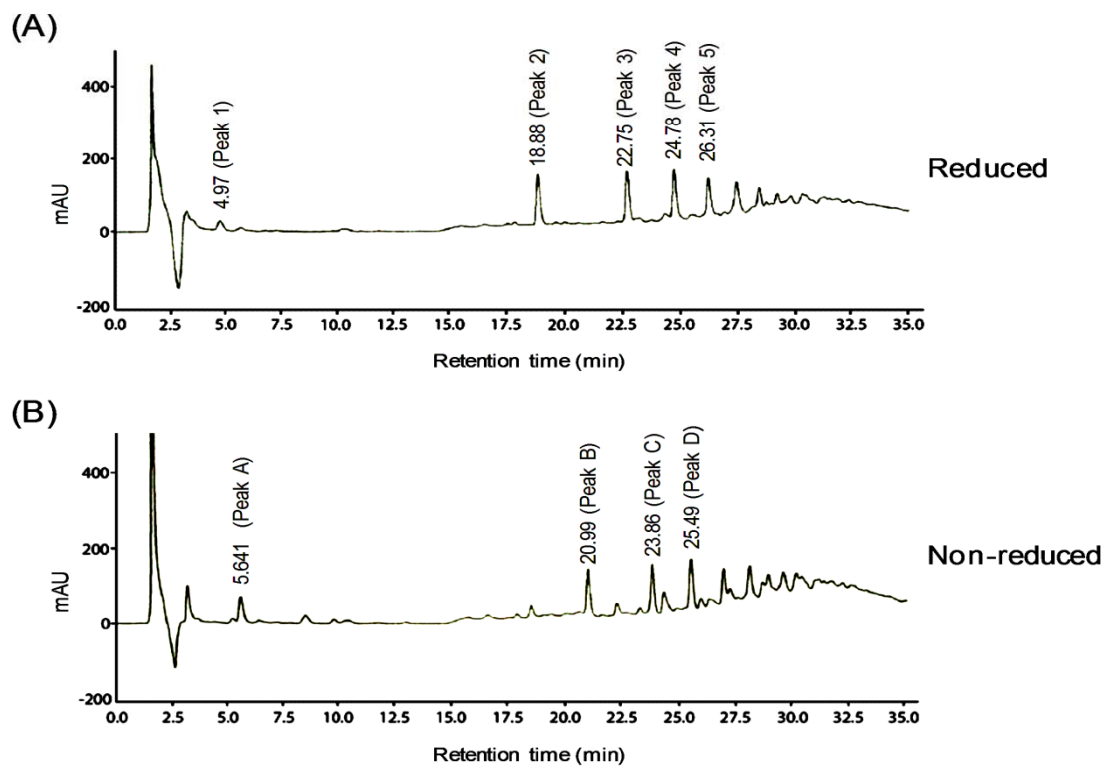


FIGURE. 2.

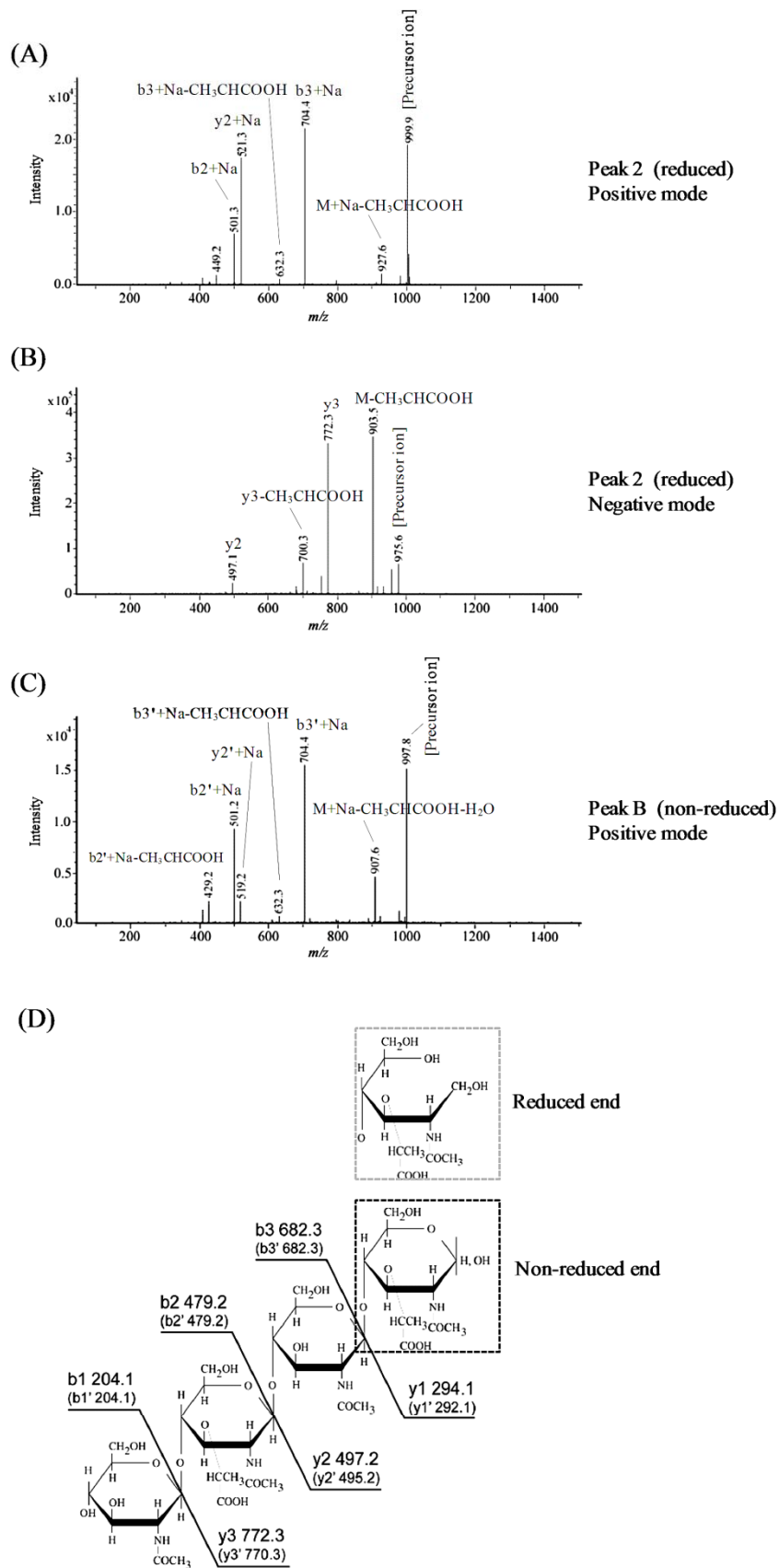


FIGURE 3.



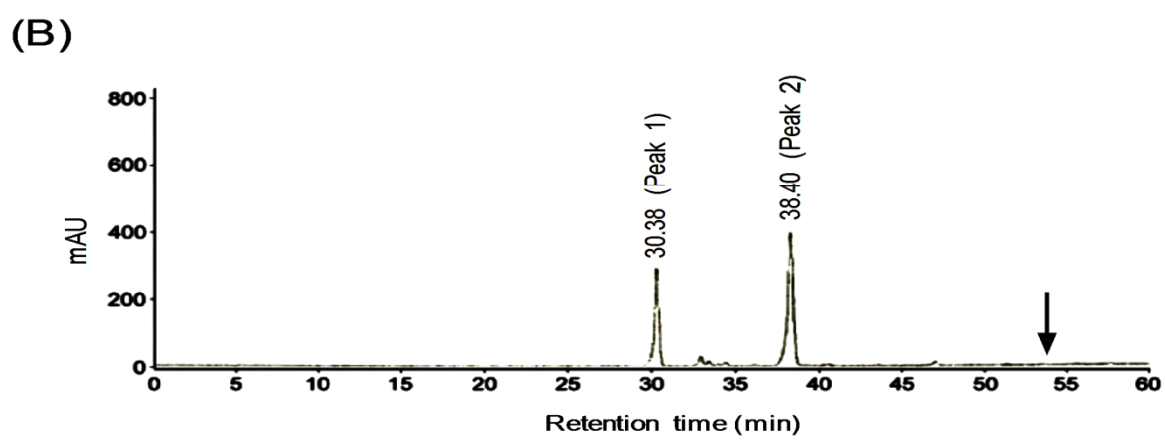
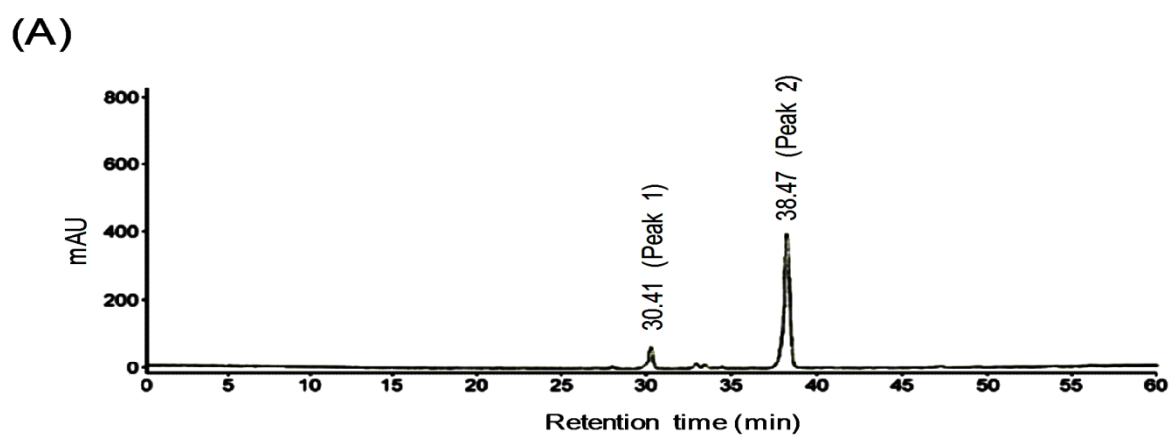
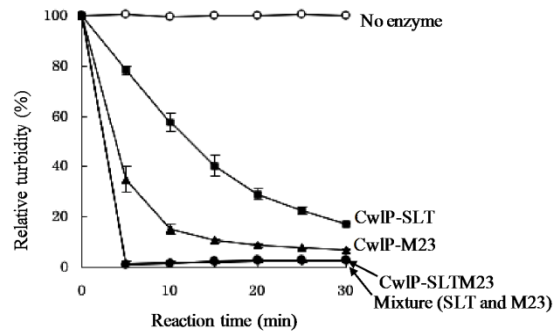


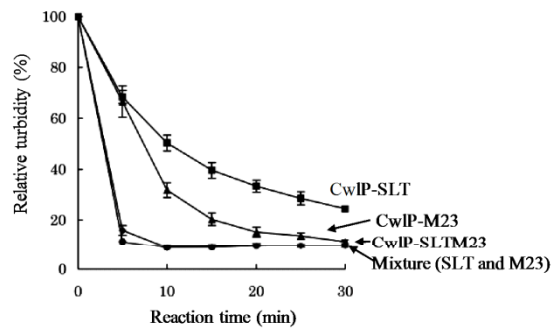
FIGURE. 5.



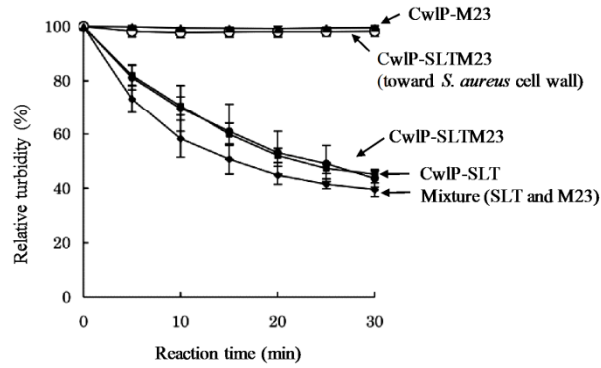
(A) *B. subtilis* cell wall



(B) *B. subtilis* peptidoglycan



(C) *S. aureus* peptidoglycan



(D) *S. thermophilus* peptidoglycan

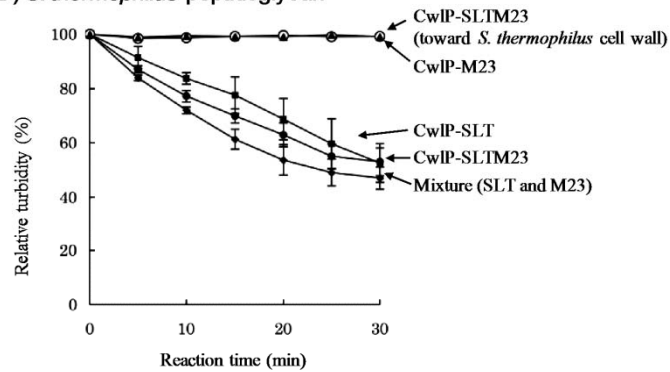


FIGURE. 7.